

Supporting Information

Carboxylic acid isomer-directed synthesis of CdS nanocluster isomers

Jing Zhang,^{*a} Yu Liu,^a Mingyang Liu,^c Zhenzhu Wang,^a Ting Qi,^d Mingming Zhang,^b Hao, shi,^{*a} and Jun Song^{*b}

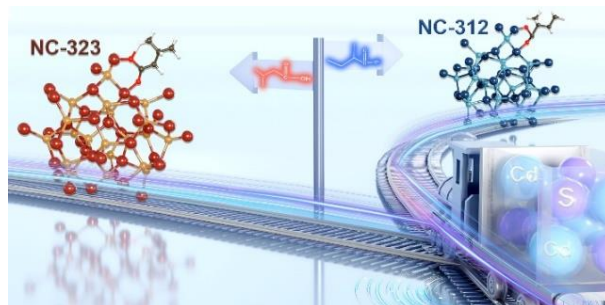
^aCollege of Materials and Chemistry & Chemical Engineering, Chengdu University of Technology, Chengdu 610059, P. R. China

^bKey Laboratory of Optoelectronic Devices and Systems of Ministry of Education and Guangdong Province, College of Physics and Optoelectronic Engineering, Shenzhen University, Shenzhen 518060, P. R. China

^cInstitute of Chemical Sciences and Engineering, Ecole Polytechnique Fédérale de Lausanne (EPFL), 1015 Lausanne, Switzerland

^dAntibiotics Research and Re-evaluation Key Laboratory of Sichuan Province, Sichuan Industrial Institute of Antibiotics, School of Pharmacy, Chengdu University, Chengdu 610106, P. R. China

J. Z. (email: zhangj0318@cdut.edu.cn) or to H. S. (email: haoshi@cdut.edu.cn) or to J. S. (email: songjun@szu.edu.cn)



Experimental Section	S2
Figure S1. Absorption spectrum of synthesized and purified NC-312 and NC-323	S6
Figure S2. TGA analysis of synthesized CdS NC-312 and NC-323	S7
Figure S3. Comparison of thermal stability of CdS NCs and reported MSCs	S8
Figure S4. Absorption evolution of NC-312 and NC-323 without adding acids	S9
Figure S5. Absorption evolution of NC-323 to NC-312 isomerization in glovebox.	S10
Figure S6. The addition amount of the isomeric acids effect on the isomerization	S11
Figure S7. Activation energies of isomerization between NC-312 and NC-323	S12
Figure S8. The comparison of coordination capacity between 2-MA and 3-MA	S13
Figure S9. DFT calculation study of Cd(2-MA) ₂ and Cd(3-MA) ₂ molecules	S14
Figure S10. The computed absorption spectra of CdS clusters with two acids capped	S15
Figure S11. FTIR spectra of NC-312 to NC-323 and NC-323 to NC-312 isomerization	S16
References	S17

Experimental Section

Chemicals

Cadmium oxide (CdO, 99.99%), oleic acid (OA, 90%), 2-methylbutyric acid (2-MA, 98%), 3-methylbutyric acid (3-MA, 99%), *n*-hexanoic acid (99%), 2-methylhexanoic acid (99%), 1-octadecene (1-ODE, 90%), and sulfur powder (S, 99.5%) were purchased from Sigma Aldrich. 2-ethylbutyric acid (99%) and 5-methylhexanoic acid (98%) were purchased from Aladdin. Hexane (CH, 99.9 %) and toluene (Tol, 99.5%) were purchased from Chengdu Kelong Chemical. Isopropanol (*i*-PrOH, 99.5%) was purchased from Macklin. All the chemicals were used as received.

Direct Synthesis of CdS NC-312 and NC-323

In a typical synthesis (Figure 1), CdO (0.0770 g, 0.60 mmol), OA (0.3730 g, 1.32 mmol), and ODE (4.5453 g) were loaded in a 50 mL three-necked flask and degassed for 30 min at room temperature. Afterwards, the mixture was heated to 240 °C under N₂ atmosphere to obtain a transparent solution with a light-yellow color. Subsequently, the solutions were cooled to 120 °C and degassed for 30 min. The resulting Cd(OA)₂ solutions were cooled to 90 °C with the addition of S powder (0.0048 g, 0.15 mmol) and 190 μL (1.75 mmol) of 2-MA or 3-MA under N₂. Then, the reaction mixture was heated to 180 °C for the synthesis of NC-312 or NC-323, respectively.

For the generality (Figure 4), the above synthetic method was applied with a slight modification. The resulting Cd(OA)₂ solutions were cooled to 90 °C with the addition of S powder (0.0048 g, 0.15 mmol) under N₂. Then, the reaction mixture was heated to 180 °C and kept for 10 min with one sampling. Meanwhile, 110 μL (0.875 mmol) of 2-ethylbutyric acid or *n*-hexanoic acid, 250 μL (1.75 mmol) of 2-methylhexanoic acid or 5-methylhexanoic acid were added to the pre-heated precursor solutions at 180 °C for the synthesis of NC-312 and NC-323, respectively.

For stability comparison between our synthesized NCs and reported MSCs (Figure S3), OA capped MSCs were synthesized by the reported two-step method.¹ In brief, Cd(OA)₂ and S powder were mixed in ODE with a feed molar ratio of 4 to 1. The reaction mixture was

heated to 180 °C for 10 min to prepare an induction period sample. In the second step, the induction period sample was incubated at 4 °C and 25 °C for one day for the formation of MSC-311 and MSC-322, respectively. Afterwards, the obtained MSC samples were transferred to 180 °C for sampling.

Isomerization between NC-312 and NC-323

For the isomerization between NC-312 and NC-323 (Figure 2 and S6), 2.0 mL of as-synthesized NC-312 or NC-323 were mixed with different amount of 3-MA or 2-MA (such as 76 μ L and 228 μ L) at 25 °C in air, respectively. Then, aliquots (25 μ L) were extracted from the mixture at different time periods and dispersed in 3.0 mL of hexane for absorption measurements. The NC-323 to NC-312 isomerization was also performed at 25 °C in glovebox (Figure S5).

Purification and Characterization

Except for Ultraviolet-visible absorption spectroscopy, all the NC samples were purified for characterization. The as-synthesized NCs were dispersed in toluene with adding of isopropanol for precipitation. Then, the solutions were centrifuged at 8500 rpm for 5 min and the supernatant was removed. The process was repeated two times and the precipitate were stored under vacuum for further characterization.

Ultraviolet-visible absorption spectroscopy (UV)

UV-visible absorption spectra were collected with 1 nm data collection interval by a SHIMADZU UV-1780 UV-visible spectrophotometer. 25 μ L of each sample was dispersed in 3.0 mL hexane for absorption measurements.

Powder X-ray diffraction (XRD)

XRD patterns were recorded on an X-ray diffractometer (Ultima IV) with a Cu K α beam ($\lambda = 1.5418 \text{ \AA}$) at 40 kV and 40 mA. The purified samples were dispersed in hexane and deposited on a silicon substrate. The patterns were collected between 10 and 80 in the 2 θ mode.

Matrix assisted laser desorption ionization-time off light mass spectrometry (MALDI-TOF MS)

The MALDI-TOF data were collected on a Autoflex speed (Bruker) mass spectrometry. [(trans-2-[3-(4-tert-Butylphenyl)-2-methyl-2-propenylidene]malononitrile (DCTB) was used to prepare the matrix solution (10 mg DCTB in 0.5 mL toluene). The matrix solution and sample dispersion (10 μ L of sample dispersed in 500 μ L of toluene) were mixed with 1 to 1 volume ratio and dropped into the sample plate.

Transmission electron microscopy (TEM)

TEM images were obtained on a HITACH HT7700 TEM. The purified samples were dispersed in toluene and dropped on a carbon coated copper grid with dried under ambient condition for TEM characterization.

X-ray photoelectron spectroscopy (XPS)

XPS measurements were performed using a K-Alpha+ XPS spectrometer (Thermos Fisher). The purified NC-312 and NC-323 were dispersed in toluene and dropped on silicon wafer for further characterization.

Thermogravimetric Analysis (TGA)

TGA experiments were performed on TGA Q50 (TA) under N₂, with the temperature increase of 10 $^{\circ}$ C/min from room temperature to 700 $^{\circ}$ C. The purified samples were dried under vacuum for one night at room temperature.

Fourier-Transform Infrared Spectroscopy (FTIR). FTIR spectra were acquired in the transmission mode using a Thermo Scientific Nicolet iS20 spectrometer. The samples were prepared by grounding the mixture of the purified NCs and KBr powders. All spectra were collected between 400-4000 cm^{-1} with a resolution of 0.5 cm^{-1} .

Computation

The study of Cd(2-MA)₂ and Cd(3-MA)₂ molecules (Figure S7) and the calculated absorption spectra of NC-312 and NC-323 (Figure 3 and S8) were performed with the Vienna ab initio Simulation Package (VASP)² within the frame of density functional theory (DFT). The structural model of pristine CdS cluster is suggested as the well-established In₃₇P₂₀ cluster with replacing In and P atoms to Cd and S.³ Furthermore, we used a pseudo-hydrogen approximation to passivate the dangling bonds on the surface of structural models.⁴⁻⁶ The exchange-correlation interactions of electron were described via the generalized gradient approximation (GGA) with PBE functional,⁴ and the projector augmented wave (PAW) method⁵ was used to describe the interactions of electron and ion. Additionally, the DFT-D3 method^{6,7} was used to account for the long-range van der Waals forces present within the system. The Monkhorst-Pack scheme⁸ was used for the integration in the irreducible Brillouin zone. The kinetic energy cut-off of 450 eV was chosen for the plane wave expansion. In order to establish an isolated environment, we put cluster models into a 30×30×30 Angstrom box in all our calculations. The lattice parameters and ionic position were fully relaxed, and the total energy was converged within 10⁻⁵ eV per formula unit. The final forces on all ions are less than 0.02/Å. For absorption calculations, the frequency-dependent dielectric matrix methodology was employed.

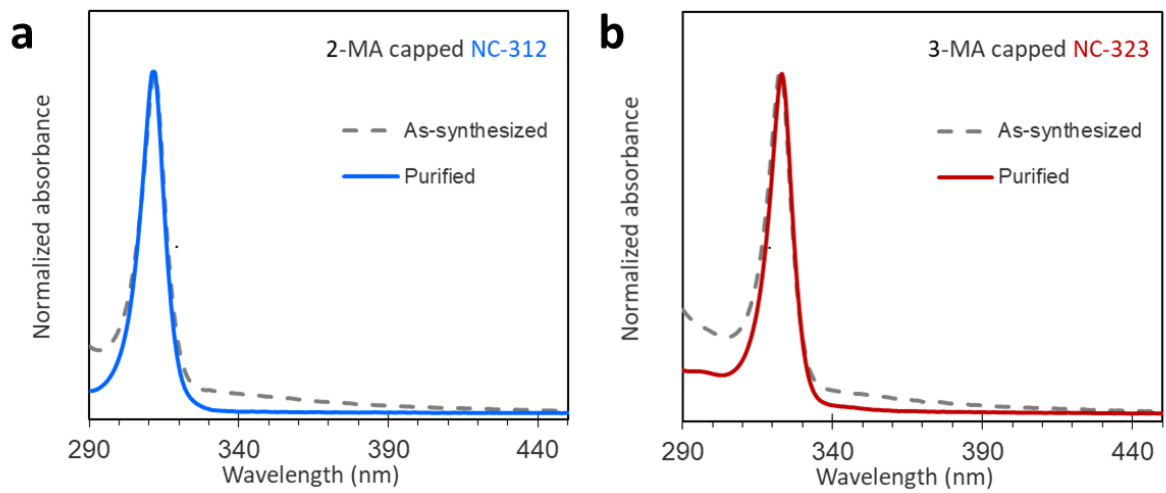


Fig. S1 UV-vis absorption spectra of as-synthesized (dash line) and purified (solid line) NC-312 (a) and NC-323 (b).

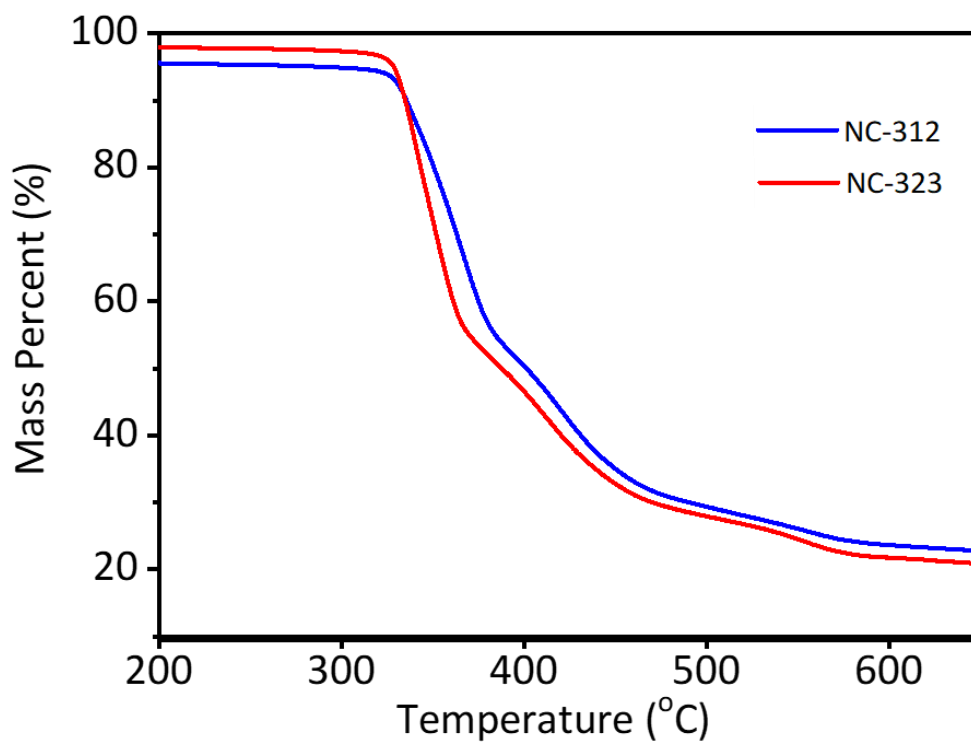


Fig. S2 TGA study of 2-MA capped NC-312 and 3-MA capped NC-323. The result suggests that the weight ratios of organic ligands to inorganic cores were 75.75 to 24.25 for NC-312, and 77.92 to 22.08 for NC-323, respectively. The difference is within the experimental error of the instrument.

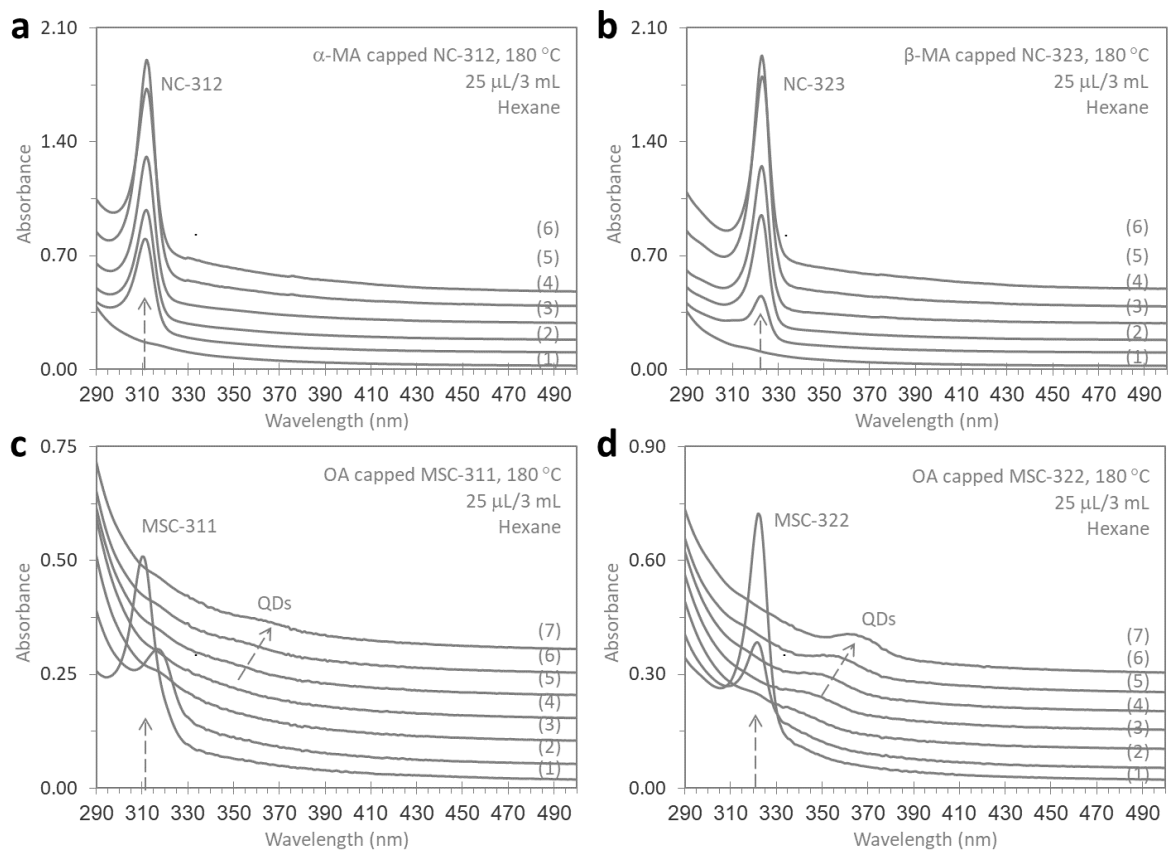


Fig. S3 (Top panel) Absorption spectral evolution of our synthesized NC-312 (a) and NC-323 (b) at 180 °C. Samples were extracted at reaction time of (1) 10 min, (2) 15 min, (3) 25 min, (4) 40 min, (5) 70 min, and (6) 130 min. (Bottom panel) Evolution of absorption spectra of previously reported CdS MSC-311 (c) and MSC-322 (d) at 180 °C. Samples were extracted at reaction time of (1) 0 s, (2) 30 s, (3) 1 min, (4) 2 min, (5) 3 min, (6) 5 min, and (7) 10 min.

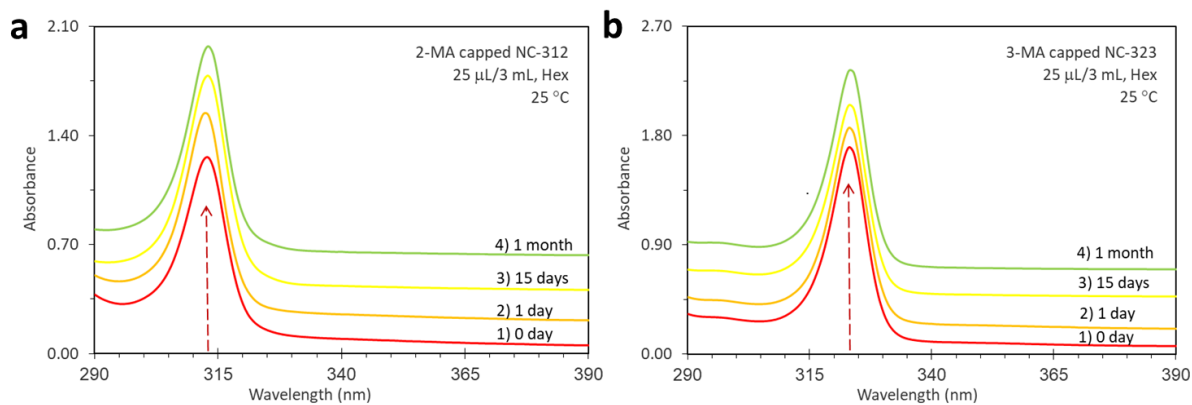


Fig. S4 The time-dependent absorption spectra of as-synthesized NC-312 (a) and NC-323 (b) stored at room temperature in air. Obviously, NC-312 and NC-323 were stable without the conversion to other NC species or QDs during the whole storage process.

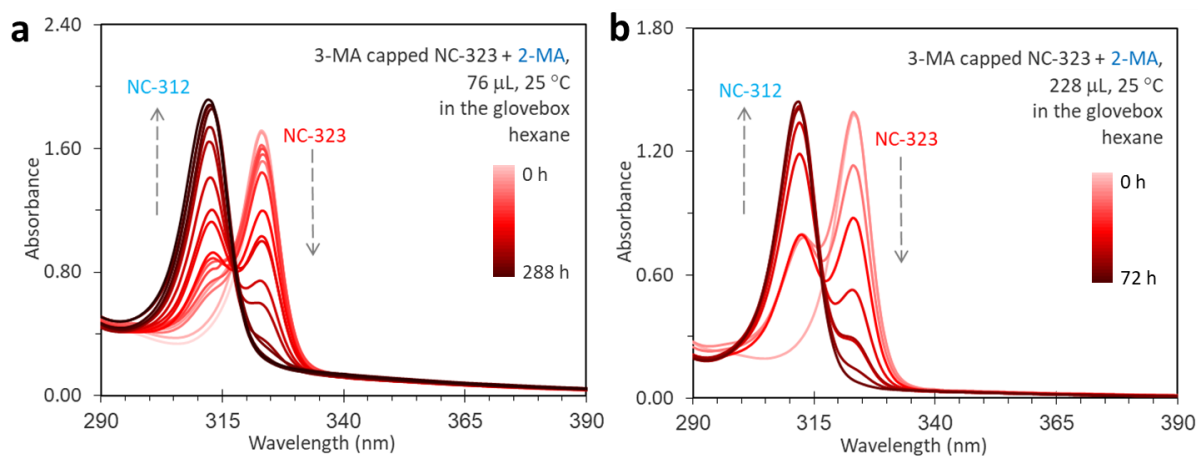


Fig. S5 Absorption spectral evolution for the isomerization from NC-323 to NC-312 at 25 °C in glovebox. 2.0 mL of as-synthesized NC-323 was mixed with 76 μL (a) or 228 μL (b) of 2-MA. Aliquots (25 μL) were taken from the mixture by time and dispersed in hexane (3 mL) for absorption measurement. The spectral collection had a 24 h interval up to 144 h and a 12 h interval until 288 h (a), and a 4 h interval up to 12 h and a 12 h interval until 72 h (b).

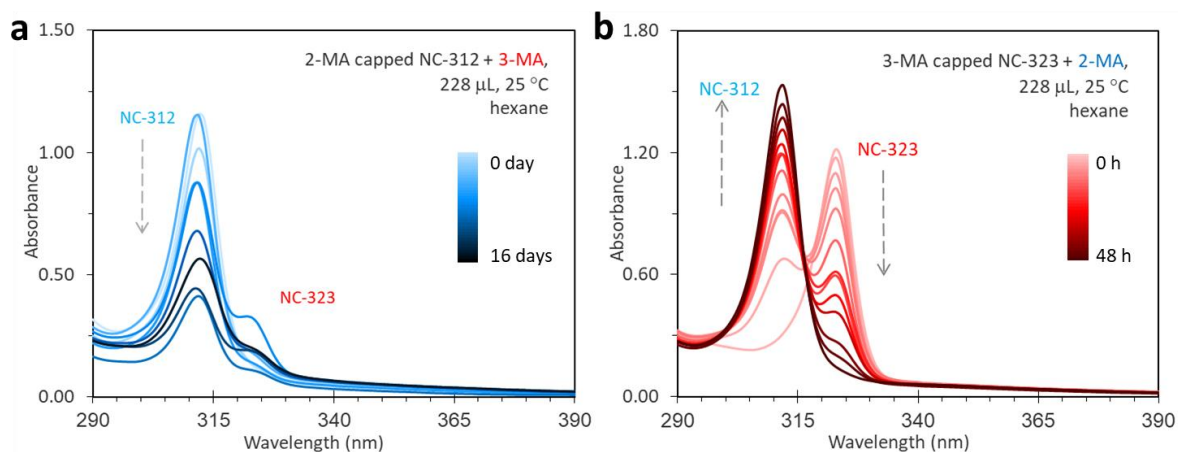


Fig. S6 Absorption spectral evolution for the isomerization between NC-312 and NC-323 at 25 $^{\circ}$ C in air. 2.0 mL of as-synthesized NC-312 (a) or NC-323 (b) were mixed with 228 μ L of 3-MA or 2-MA, respectively. Aliquots (25 μ L) were taken from the mixture by time and dispersed in hexane (3 mL) for absorption measurement. For NC-323 \Rightarrow NC-312 isomerization, the conversion rate was increased when the addition amount of 2-MA increased from 76 μ L (Figure 2b) to 228 μ L (Figure S6b). However, the isomerization from NC-312 to NC-323 was inhibited and accompanied by the decomposition of NC-312 when the addition amount of 3-MA increased from 76 μ L (Figure 2a) to 228 μ L (Figure S6a).

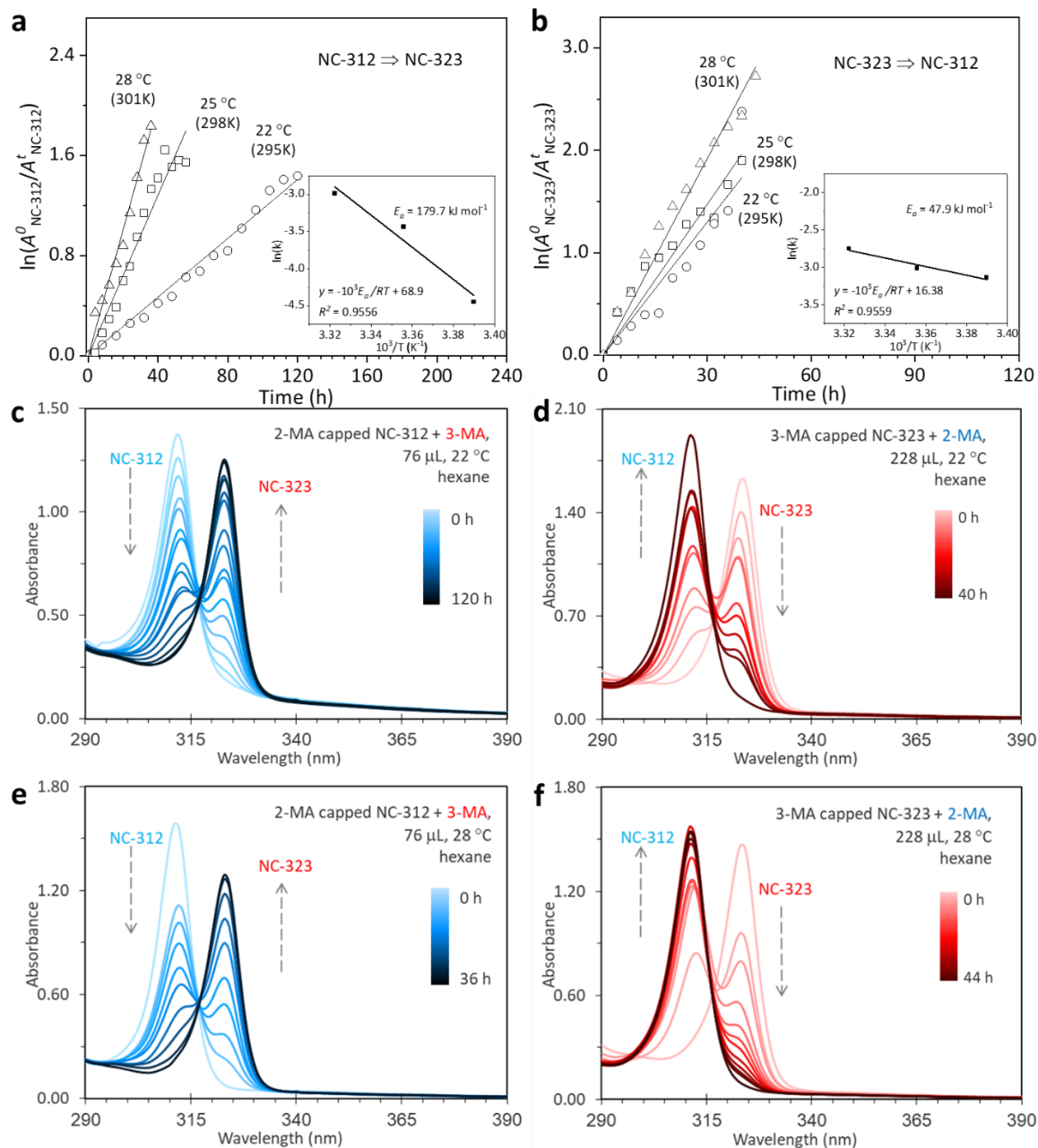


Fig. S7 First-order reaction kinetic fitting for the isomerization from NC-312 to NC-323 (a) and from NC-323 to NC-312 (b) at three temperatures as indicated. The time dependent $\ln(A^0/A^t)$ was fitted by first-order equation $\ln(A^0/A^t) = kt$ (solid lines), where A^0 is the initial absorbance of the reactants, A^t is the time-dependent absorbance of the reactants. The slopes correspond to the rate constants k (h⁻¹). The insets show the Arrhenius plot, with a y axis of $\ln(k)$ and an x axis of $1/T$. The slope of the fitted line is E_a/R , where E_a is the activation energy for the relating transformation and R is the ideal gas constant. The corresponding optical absorption spectra are shown as below(c-f).

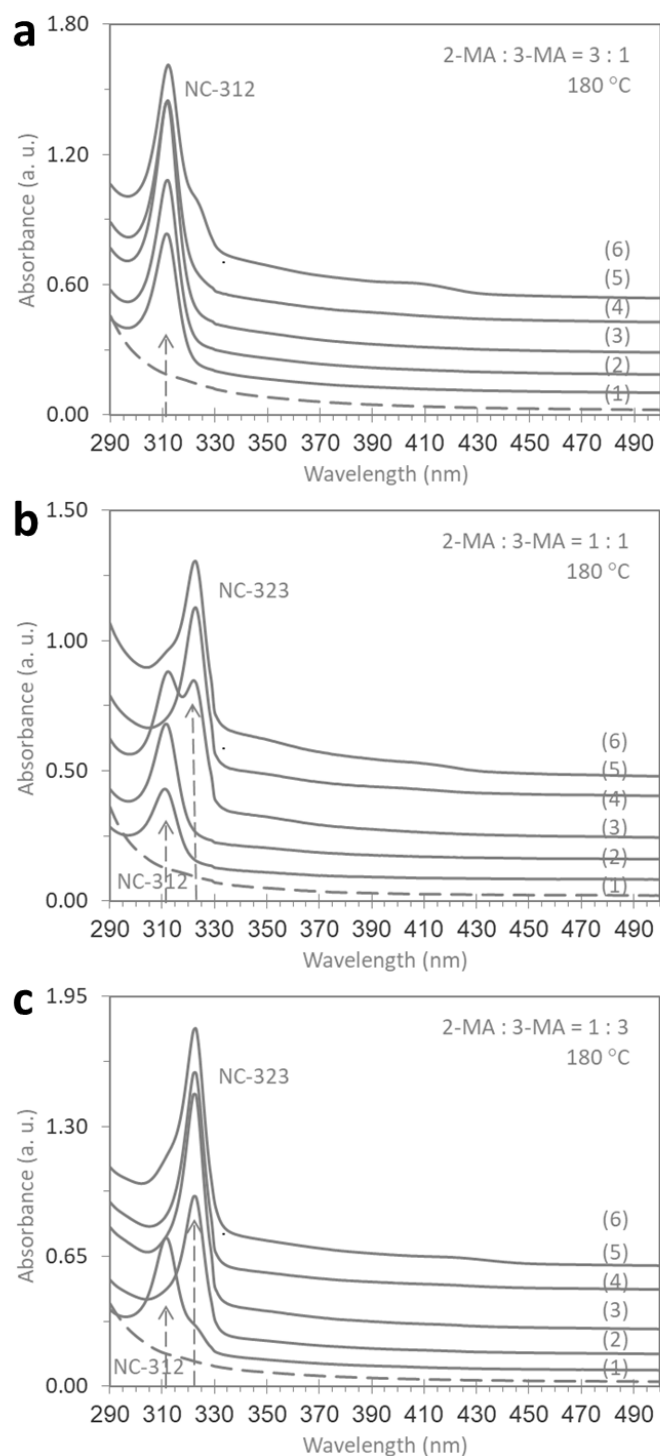


Fig. S8 Temporal evolution of absorption spectra of reactions of $\text{Cd}(\text{OA})_2 + \text{SODE}$ by adding a 2-MA and 3-MA mixture with a total volume of $190 \mu\text{L}$. The different ratio of 2-MA to 3-MA in the mixture as shown in the inset. One sample was extracted at $180 \text{ }^\circ\text{C}$ for 10 min (1) before the addition of acids. After the addition, five samples were extracted at $180 \text{ }^\circ\text{C}$ for the reaction time of (2) 5 min, (3) 15 min, (4) 30 min, (5) 60 min, and (6) 120 min.

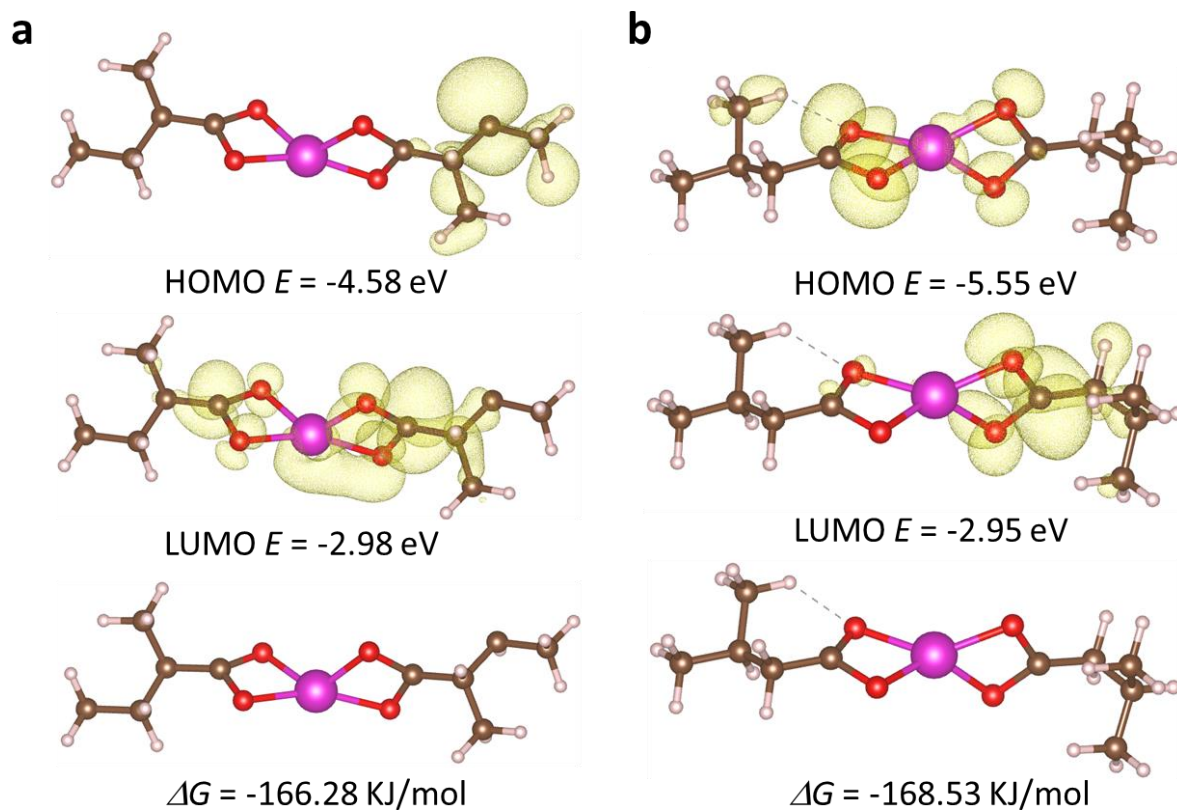


Fig. S9 DFT calculation study of Cd(2-MA)₂ (a) and Cd(3-MA)₂ (b) molecules. The highest occupied molecular orbitals (HOMO, top panel) and lowest unoccupied molecular orbitals (LUMO, middle panel), with their energy (eV) are indicated. The bottom panel shows the Gibbs free energy ΔG of Cd(2-MA)₂ and Cd(3-MA). The lower ΔG of Cd(3-MA)₂ than that of Cd(2-MA)₂ suggests that 3-MA has stronger coordination ability to Cd than 2-MA, resulting in the higher stability of Cd(3-MA)₂.

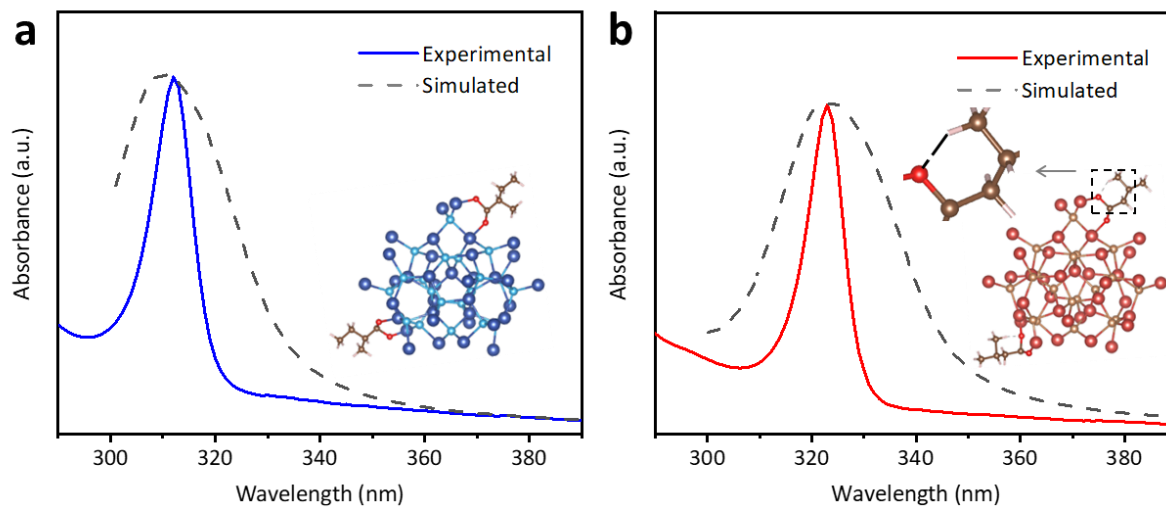


Fig. S10 Comparison of the experimental (solid line) and calculated (dash line) absorption spectra of CdS NC-312 (a) and NC-323 (b). The inset shows the models of pristine Cd₃₇S₂₀ clusters with two 2-MA or 3-MA coordinated. In the presence of 2-MA and 3-MA, the computed absorption peak shifted to 311.9 nm and 321.4 nm, respectively.

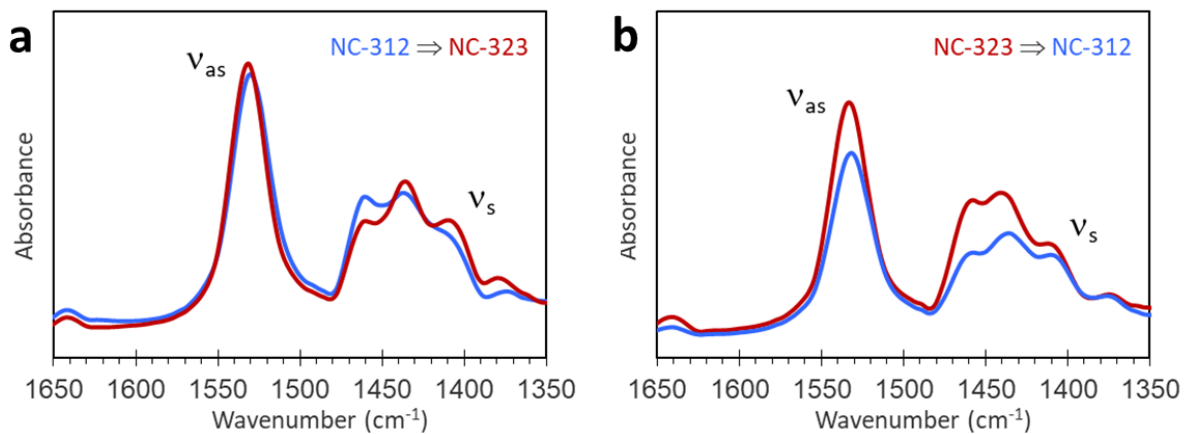


Fig. S11 FTIR spectra of the carboxyl asymmetric (ν_{as}) and symmetric (ν_s) stretches of, (a) as-synthesized NC-312 (blue line) and NC-323 transformed from NC-312 with adding 3-MA (red line), (b) as-synthesized NC-323 (red line) and NC-312 transformed from NC-323 by adding 2-MA (blue line). For (a) and (b), the difference (Δ) between the carboxylate asymmetric stretches (ν_{as}) and symmetric stretches (ν_s) are 122 cm^{-1} and 121 cm^{-1} , indicating a chelating bidentate configuration.⁹

References

- 1 B. Zhang, T. Zhu, M. Ou, N. Rowell, H. Fan, J. Han, L. Tan, M. T. Dove, Y. Ren, X. Zuo, S. Han, J. Zeng and K. Yu, *Nat. Commun.*, 2018, **9**, 2499.
- 2 G. Kresse and J. Furthmüller, *Phys. Rev. B*, 1996, **54**, 11169-11186.
- 3 D. C. Gary, S. E. Flowers, W. Kaminsky, A. Petrone, X. Li and B. M. Cossairt, *J. Am. Chem. Soc.*, 2016, **138**, 1510-1513.
- 4 J. P. Perdew, K. Burke and M. Ernzerhof, *Phys. Rev. Lett.*, 1996, **77**, 3865-3868.
- 5 G. Kresse, D. Joubert, *Phys. Rev. B*, 1999, **59**, 1758-1775.
- 6 S. Grimme, J. Antony, S. Ehrlich and H. Krieg, *J. Chem. Phys.*, 2010, **132**, 154104.
- 7 S. Grimme, S. Ehrlich and L. Goerigk, *J. Comput. Chem.*, 2011, **32**, 1456-1465.
- 8 D.J. Chadi, *Phys. Rev. B*, 1977, **16**, 1746-1747.
- 9 C. B. Williamson, D. R. Nevers, A. Nelson, I. Hadar, U. Banin, T. Hanrath and R. D. Robinson, *Science*, 2019, **363**, 731-735.